



## A GROUND MOTION SIMULATION COUPLED WITH AN EIKONAL SOLVER AND ITS APPLICATION WITH A FORMULA USING ISOCHRONES JUMPING INTENSITY

R. Imai<sup>(1)</sup>, M. Yamada<sup>(2)</sup>, K. Hada<sup>(3)</sup>, H. Fujiwara<sup>(4)</sup>

<sup>(1)</sup> Ph.D, Mizuho Information & Research Institute, Inc., ryuta.imai@mizuho-ir.co.jp

<sup>(2)</sup> Ph.D, NEWJEC Inc., yamadams@newjec.co.jp

<sup>(3)</sup> Msc, NEWJEC Inc., hadakj@newjec.co.jp

<sup>(4)</sup> Ph.D, National Research Institute for Earth Science and Disaster Prevention, fujiwara@bosai.go.jp

### **Abstract**

We describe three achievements for a ground motion simulation. First, we propose a kinematic modeling in which rupture delay time is governed by an eikonal equation on Riemannian manifold and develop a coupling method between the eikonal solver and a ground motion simulation. In general the rupture delay time is depending on the fault shape. So we derive the equation by considering the Riemannian metric of the fault surface and give a detailed discretization of its difference scheme to deal with a curved surface fault. Next, in order to explain the effect of spatially discontinuous non-uniformity of rupture velocity, we introduce an isochrones jumping intensity and obtain a new decomposed isochrones formula with mathematical rigor. It is known that the representation theorem with the Green's function can be rewritten into an expression with a contour integral by the isochrones theory. The new formula says that the known isochrones formula for velocity can be decomposed into a trend component and a disturbance component. The disturbance component consists of the isochrones jumping intensity. Finally, by applying our ground motion simulation coupled with the eikonal solver and the decomposed isochrones formula, we investigate some relations between the non-uniformity of the rupture velocity and pulse-like disturbance of the ground motion velocity. Our simulations show that the disturbance of velocity waveform corresponds with that of rate of change of isochrones band area. It turns out that the pulse-like disturbance of velocity waveform occurs when isochrones move across the region where rupture velocity varies discontinuously. Thus we can explain that the pulse-like disturbance of the ground motion velocity occurs when the isochrones jumping intensity has nonzero value. We, however, think that further discussion with respect to the decision of rupture velocity is required. So we would like to study the dynamic rupture model in order to understand how to give the spatial distribution of rupture velocity in future works.

*Keywords: ground motion simulation, eikonal solver on Riemannian manifold, isochrones jumping intensity*

## 1. Introduction

Rupture propagation process is an important factor for ground motion on very near site from active faults. Actual faults are not flat and have curved shapes. Their rupture propagation is spatially non-uniform and its velocity is distributed discontinuously. Thus such realistic kinematic modeling for ground motion simulation is required increasingly. In our research we propose a kinematic modeling with which we can consider both a curved surface and spatially discontinuous non-uniformity of rupture velocity. Especially we develop an eikonal solver on Riemannian manifold and a coupling method between the eikonal solver and a ground motion simulation. Moreover we introduce an isochrones jumping intensity and extend a known isochrones formula to obtain a new decomposed formula. Using our coupling method and isochrones formula, we investigate some relations between pulse-like disturbance of ground motion and non-uniform rupture process.

In many practical ground motion predictions, a kinematic modeling approach has been used because of its numerical simplicity. In the kinematic modeling approach, a slip velocity function is important and many functions have been proposed so far. [1][2] The slip velocity function modeling can give a detailed slip process at every source point, but it says nothing with respect to the spatially non-uniformity of rupture velocity. Real fault surfaces are not necessarily flat and may bend and have curved shapes. This is why we propose a kinematic modeling with which we can consider both a curved surface fault and spatially discontinuous non-uniformity of rupture velocity. In our modeling we assume that rupture propagation is governed by an eikonal equation in a curved space. We derive the equation on a two dimensional Riemannian manifold so that we can deal with a curved surface faults. Then we develop the eikonal solver on Riemannian manifold and construct a coupling method between the eikonal solver and the ground motion simulation.

In discussion with our coupling method, a concept of the isochrones is effective. [3][4][5] The isochrones formula plays an important role in our research, but their derivation in a general setting seems to be not trivial. So we give a derivation of the isochrones formula. Moreover we introduce an isochrones jumping intensity in order to give theoretical discussions for pulse-like disturbance of ground velocity. Using the isochrones jumping intensity we extend the isochrones formula to obtain a new decomposed expression of it. Our decomposition of the isochrones formula for velocity waveform consists of two components, that is, a trend component and a disturbance component. Then it turns out that the disturbance component can be expressed by means of the isochrones jumping intensity. Using the disturbance component of the isochrones formula for velocity waveform, we can explain some correspondence between pulse-like disturbance of ground velocity and spatially discontinuous non-uniformity of rupture process.

## 2. Methods

### 2.1 Eikonal solver

The eikonal equation on a Riemannian manifold was mentioned in such field as computer vision and image processing. [6][7][8] In the aim to target the rupture propagation on a curved surface fault, we derive the eikonal equation over a two dimensional Riemannian manifold. We recall some terminologies about two dimensional Riemannian manifold  $M$  imbedded into the three dimensional Euclidean space  $R^3$ . We let  $\varphi: \rightarrow M \subset R^3$  be an inverse of local coordinates, where  $D \subset R^2$  is an open set. Then  $g_1 = \frac{\partial \varphi}{\partial \xi^1} \in R^3$  and  $g_2 = \frac{\partial \varphi}{\partial \xi^2} \in R^3$  are covariant base vectors and their standard inner product  $g_{ij} = (g_i, g_j)$  defines the Riemannian metric. We let a matrix  $g^{-1} = (g^{ij})$  be the inverse matrix of  $g = (g_{ij})$ . Then  $g^i = \sum_j g^{ij} g_j$  are contravariant base vectors and the gradient  $\nabla T$  of the rupture delay time  $T$  is defined as follows:

$$\nabla T = \sum_i \frac{\partial T}{\partial \xi^i} g^i = \sum_j \left( \sum_i g^{ij} \frac{\partial T}{\partial \xi^i} \right) g_j. \quad (1)$$

Therefore the eikonal equation on a Riemannian manifold is described by

$$g^{11} \left( \frac{\partial T}{\partial \xi^1} \right)^2 + 2g^{12} \left( \frac{\partial T}{\partial \xi^1} \right) \left( \frac{\partial T}{\partial \xi^2} \right) + g^{22} \left( \frac{\partial T}{\partial \xi^2} \right)^2 = \frac{1}{v_r(\xi)^2} \quad (\xi \in D), \quad (2)$$

$$T(\eta) = 0 \quad (\eta \in \varphi^{-1}(R)),$$

where  $R \subset M$  is a set of hypocenters. We may note that the metric  $g^{12}$  vanishes if the fault considered is flat and that Eq. (2) generalizes the standard eikonal equation. We apply the Fast Marching Method ([6][7]) in order to solve the eikonal equation Eq. (1). By a small modification of the upwind discretization for the usual eikonal equation [6], we can construct our upwind discretization for the eikonal equation on a Riemannian manifold. For any grid point  $(m, n)$ , we let  $\alpha = \min\{T_{m-1,n}, T_{m+1,n}\}$  and  $\beta = \min\{T_{m,n-1}, T_{m,n+1}\}$ . Then our discretization is as follows. (for only the case of  $\alpha < \beta$ )

$$g^{11} \left( \frac{T_{m,n} - \alpha}{\Delta \xi^1} \right)^2 + 2g^{12} s_{m,n} t_{m,n} \left( \frac{T_{m,n} - \alpha}{\Delta \xi^1} \right) \left( \frac{T_{m,n} - \beta}{\Delta \xi^2} \right) + g^{22} \left( \frac{T_{m,n} - \beta}{\Delta \xi^2} \right)^2 = \frac{1}{(v_r)_{m,n}^2} \quad (\beta < T_{m,n}),$$

$$g^{11} \left( \frac{T_{m,n} - \alpha}{\Delta \xi^1} \right)^2 = \frac{1}{(v_r)_{m,n}^2} \quad (\alpha < T_{m,n} < \beta), \quad (3)$$

$$s_{m,n} = \begin{cases} +1 & (T_{m-1,n} \leq T_{m+1,n}) \\ -1 & (T_{m-1,n} > T_{m+1,n}) \end{cases}, \quad t_{m,n} = \begin{cases} +1 & (T_{m,n-1} \leq T_{m,n+1}) \\ -1 & (T_{m,n-1} > T_{m,n+1}) \end{cases}$$

It may be remarked that the Riemannian metric  $(g_{ij})_{m,n}$  at the grid point  $(m, n)$  can be calculated in such a way that  $(g_{ij})_{m,n} = \left( \left( \frac{\partial \varphi}{\partial \xi^i} \right)_{m,n}, \left( \frac{\partial \varphi}{\partial \xi^j} \right)_{m,n} \right)$  when the position vector  $\varphi(\xi)$  of the fault surface at every grid point in a local coordinate plane is given.

## 2.2 Coupling method between ground motion simulation and eikonal solver

We aim to reveal some relations between the rupture process of near-field earthquakes and the ground motions. So, a simple model which can deal with a body wave is preferable. In this paper, we concentrate our attention upon ground motions induced by a body wave in whole three dimensional elastic media. Then it is well-known that the representation theorem with the Green's function leads us to the following: [9]

$$u_n(x, t) = \int_S dS(\xi) \int_{-\infty}^{+\infty} m_{kl}(\xi, s) \frac{\partial G_{nk}}{\partial \xi_l}(x, t - s; \xi, 0) ds, \quad (4)$$

where  $u_n(x, t)$  is a displacement of an observation point  $x$  at a time  $t$ ,  $m_{kl}(\xi, s)$  is a seismic moment density tensor at a single source point  $\xi$  and a time  $s$  and  $G_{nk}(x, t; \xi, s)$  is the Green's function for receiver  $(x, t)$  and source  $(\xi, s)$ . Then, by substituting the explicit formula of the Green's function for a double couple point source into Eq. (4), we have that

$$u_n(x, t) = \frac{1}{4\pi\rho} \left\{ \begin{aligned} & \int_S \frac{R_n^N}{r^4} m\tilde{F}(x, t, \xi) dS + \int_S \frac{R_n^{IP}}{\alpha^2 r^2} mF \left( t - \frac{r}{\alpha} - \frac{r'}{v_r} \right) dS + \int_S \frac{R_n^{IS}}{\beta^2 r^2} mF \left( t - \frac{r}{\beta} - \frac{r'}{v_r} \right) dS \\ & + \int_S \frac{R_n^{FP}}{\alpha^3 r} m\dot{F} \left( t - \frac{r}{\alpha} - \frac{r'}{v_r} \right) dS + \int_S \frac{R_n^{FS}}{\beta^3 r} m\dot{F} \left( t - \frac{r}{\beta} - \frac{r'}{v_r} \right) dS \end{aligned} \right\}, \quad (5)$$

where  $\rho$  is mass density,  $r' = |\xi - \xi_0|$  is distance between a hypocenter  $\xi_0$  and a fault surface point  $\xi$ ,  $r = |x - \xi|$  is distance between an observation point  $x$  and a point  $\xi$ ,  $m$  is seismic moment density,  $\alpha$  is the velocity of the primary wave,  $\beta$  is the velocity of the secondary wave,  $v_r$  is the rupture propagation velocity and  $R_n^*$  are radiation patterns. Moreover  $\dot{F}(t)$  and  $F(t)$  represent a slip velocity function and a slip displacement function respectively and we denote  $\tilde{F}(x, t, \xi)$  as the following function.

$$\begin{aligned}\bar{F}(x, t, \xi) &= \int_{\frac{r}{\alpha}}^{\frac{r}{\beta}} sF\left(t - s - \frac{r'}{v_r}\right) ds \\ &= \frac{r}{\alpha} FI\left(t - \frac{r}{\alpha} - \frac{r'}{v_r}\right) + FII\left(t - \frac{r}{\alpha} - \frac{r'}{v_r}\right) - \frac{r}{\beta} FI\left(t - \frac{r}{\beta} - \frac{r'}{v_r}\right) - FII\left(t - \frac{r}{\beta} - \frac{r'}{v_r}\right),\end{aligned}\quad (6)$$

where  $FI(t) = \int_0^t F(a)da$  and  $FII(t) = \int_0^t FI(a)da = \int_0^t da \int_0^a F(b)db$  are indefinite integrals respectively. Now we divide the fault surface  $S$  into a finite disjoint union  $S = \cup_n S_n$  of small meshes  $S_n$  and chose points  $\xi_n \in S_n$  in all meshes. We evaluate the right hand term in Eq. (5) at every mesh  $S_n$  and sum them into Eq. (5) over the fault surface. In evaluation of Eq. (5) at every mesh  $S_n$ , we approximate it by the value of the integrand at a point  $\xi_n \in S_n$  and the area of  $S_n$ .

Our purpose is to deal with the non-uniform rupture propagation velocity in ground motion simulations. So we couple the eikonal solver, which solves the eikonal equation to calculate the rupture delay time  $T(\xi)$ , with the ground motion simulation. That is, in Eq. (5), we may substitute the rupture delay time  $T(\xi)$  for  $\frac{r'}{v_r}$ .

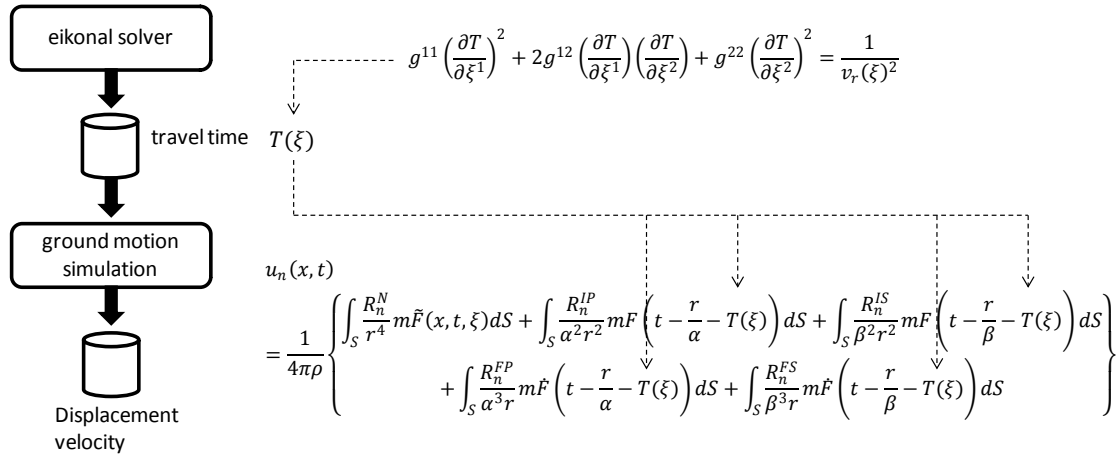


Fig.1 Coupling method between ground motion simulation and eikonal solver

### 2.3 Isochrones formula

In [3] a definition of the isochrones and a contour integral formula for ground motion displacement are given in a very simple setting. In their analysis of the stopping phase at a barrier, the isochrones theory is effectively used. In [4] and [5], the substantially same isochrones formulae are used for analysis of high-frequent ground motion. In [5] they rewrote the isochrones formula to derive a general expression for the spectral characteristics of supershear rupture. in [4] the isochrones formula for ground acceleration is investigated in detail. In our purpose, however, we need the isochrones formula for ground velocity and its disturbance component. So we give a mathematically rigorous derivation of the formula in more general settings. After that, we introduce an isochrones jumping intensity in order to give theoretical discussions for pulse-like disturbance of velocity waveform. Using the isochrones jumping intensity we extend the formula with mathematical rigor to obtain a new decomposed expression of the formula for velocity.

For a fixed observation point  $x$  and a hypocenter  $\xi_0$ , we let a delay time  $\theta(\xi)$  to be  $\theta(\xi) = \frac{r}{\alpha} + T(\xi)$  or  $\theta(\xi) = \frac{r}{\beta} + T(\xi)$ , where  $T(\xi)$  is the rupture delay time. For instance  $T(\xi) = \frac{r'}{v_r}$  in the case of uniform rupture velocity  $v_r$ . Then Eq. (5) shows that the displacement is written by a finite summation of the following forms of function.

$$u(t) = \int_S g(\xi) f(t - \theta(\xi)) dS(\xi). \quad (7)$$

In fact, the far-field component of the secondary wave shows that  $g(\xi) = \frac{R_n^{FS}}{\beta^3 r}$  and  $f(t) = \dot{F}(t)$ . Now we denote a contour curve  $C_{t-\lambda}$  of the function  $\theta(\xi)$  as

$$C_{t-\lambda} = \{\xi \in R^2; \theta(\xi) = t - \lambda\} \quad (8)$$

In what follows, we call this contour curve  $C_{t-\lambda}$  as the isochrones of the delay function  $\theta$ . If the isochrones  $C_{t-\lambda}$  are represented by a parameter description such as  $\xi = \varphi^{t-\lambda}(\lambda')$ , local coordinates transformation  $R^2 \ni (\lambda', \lambda) \mapsto (\xi_1, \xi_2) \in R^2$  can be defined.

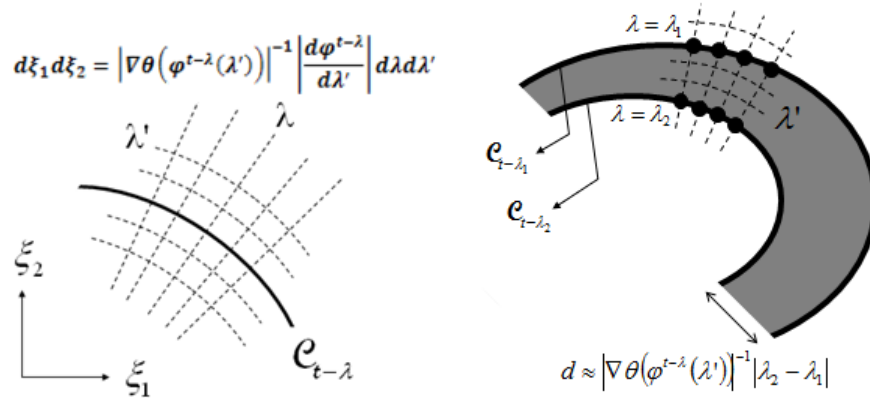


Fig 2. Local coordinates of isochrones (left) and isochrones band (right)

$\lambda'$ -curve is a contour curve of the delay function  $\theta$  and  $\lambda$ -curve is perpendicular to the  $\lambda'$ -curve. Such coordinates can be defined locally and these local coordinate patches can cover the fault plane. Isochrones band is a region surrounded by two isochrones  $C_{t-\lambda_1}$  and  $C_{t-\lambda_2}$ . Its width is proportional to  $|\nabla\theta|^{-1}d\lambda$ .

Actually we can restrict the range of  $(\lambda', \lambda)$  into the rectangular region  $[0,1] \times [\lambda_1, \lambda_2]$  and cover the fault surface by a finite union of the images of such local coordinates. The interval  $[\lambda_1, \lambda_2]$  is a support of the function  $f(\lambda)$  and the image of such local coordinates means a region between two isochrones  $C_{t-\lambda_1}$  and  $C_{t-\lambda_2}$ . We call this region  $D_{\lambda_1, \lambda_2}(t)$  as the isochrones band in this paper. It should be remarked that the Jacobian of the local coordinates transformation is as follows:

$$\left| \det \frac{\partial(\xi_1, \xi_2)}{\partial(\lambda', \lambda)} \right| = |\nabla\theta(\varphi^{t-\lambda}(\lambda'))|^{-1} \left| \frac{d\varphi^{t-\lambda}}{d\lambda'} \right|. \quad (9)$$

That is to say, the surface element  $dS = d\xi_1 d\xi_2$  can be decomposed into the arc length  $dC_{t-\lambda} = \left| \frac{d\varphi^{t-\lambda}}{d\lambda'} \right| d\lambda'$  of the isochrones and its normal directional length  $dn = |\nabla\theta(\varphi^{t-\lambda}(\lambda'))|^{-1} d\lambda$  as follows:

$$dS = dn dC_{t-\lambda}. \quad (10)$$

Then, substituting Eq. (10) into Eq. (7), we may assume that the displacement is written by a finite summation of the following forms.

$$u(t) = \int_{\lambda_1}^{\lambda_2} f(\lambda) d\lambda \int_0^1 g(\varphi^{t-\lambda}(\lambda')) |\nabla\theta(\varphi^{t-\lambda}(\lambda'))|^{-1} \left| \frac{d\varphi^{t-\lambda}}{d\lambda'} \right| d\lambda'. \quad (11)$$

For simplicity, we write  $h_{\lambda'}(t) = g(\varphi^t(\lambda')) |\nabla\theta(\varphi^t(\lambda'))|^{-1} \left| \frac{d\varphi^t}{d\lambda'} \right|$  in order to get

$$u(t) = \int_0^1 f * h_{\lambda'}(t) d\lambda', \quad (12)$$

where  $f * h_{\lambda'}(t) = \int_{\lambda_1}^{\lambda_2} f(\lambda) h_{\lambda'}(t - \lambda) d\lambda$  is a convolution of  $f$  and  $h_{\lambda'}$ . In the case of non-uniform discontinuous rupture velocity, it should be noted that  $h_{\lambda'}(t)$  is discontinuous with regard to  $t$  for every fixed  $\lambda'$ . In fact  $|\nabla\theta(\varphi^t(\lambda'))|$  is discontinuous when a point  $\xi = \varphi^t(\lambda')$  of the isochrones runs across the boundary on which rupture velocity varies discontinuously. We suppose that  $h_{\lambda'}(t)$  jumps discontinuously at  $t = \tau(\lambda')$ . Then we define the isochrones jumping intensity  $j_h(\lambda')$  as follows:

$$j_h(\lambda') = h_{\lambda'}(\tau(\lambda') + 0) - h_{\lambda'}(\tau(\lambda') - 0). \quad (13)$$

An easy calculation with Schwartz distribution theory leads us to that

$$\frac{d}{dt}(f * h_{\lambda'}) = f * \frac{dh_{\lambda'}}{dt} + j_h(\lambda')f(t - \tau(\lambda')), \quad (14)$$

where  $\frac{dh_{\lambda'}}{dt}$  stands for a classical derivative of  $h_{\lambda'}$ , defined except for discontinuous points. Therefore we obtain a new decomposed expression of the following isochrones formula:

$$\frac{du}{dt}(t) = \int_0^1 f * \frac{dh_{\lambda'}}{dt}(t) d\lambda' + \int_0^1 j_h(\lambda')f(t - \tau(\lambda')) d\lambda'. \quad (15)$$

The first term of the right hand side in Eq. (15) stands for a trend component of the ground motion velocity and the second term stands for a disturbance component. From this formula Eq. (15) it turns out that a disturbance of the ground motion velocity occurs when a point  $\xi = \varphi^t(\lambda')$  of the isochrones runs across the boundary on which rupture velocity varies discontinuously. In other words, a pulse-like disturbance of the ground velocity occurs when the isochrones jumping intensity  $j_h(\lambda')$  has nonzero value.

### 3. Simulations

#### 3.1 Directivity and numerical instability

First of all we investigate some properties of our ground motion simulation. Empirically it is known that ground motion simulation may often cause non-physical high frequent oscillations in the velocity waveform in the backward directivity regions. In this paper we refer to the non-physical high frequent oscillation as a numerical instability. We found that a simple example gives numerical instability of velocity waveform of ground motion of an observation point located in the backward directivity. The fault width and length are 20km and 40km respectively and the dip angle is 90 degree. Its depth of the upper edge is on the ground. The hypocenter is located on the lower corner and the rupture velocity is constant and uniform. Two observation points are located away 1km from the fault.

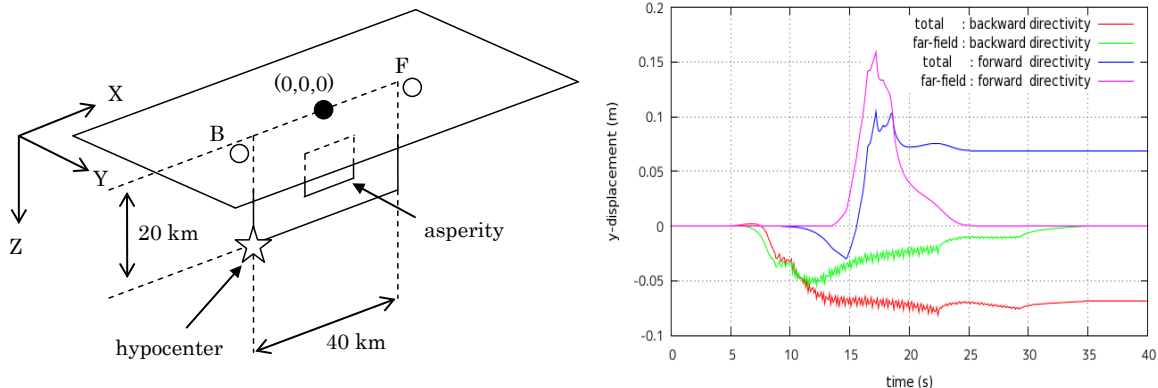


Fig 3. Fault model (left) and time histories of Y-displacement (right)

Left figure shows that two observation points are located on the plane which includes the upper edge of the fault and is perpendicular to it. It should be remarked that the only body wave in whole three dimensional elastic media is considered. Right figure shows that numerical instabilities occur on the backward directivity.

The observation point B is located on the backward directivity and another point F on the forward directivity. We set mesh size as 400m. There are almost no numerical instabilities on the observation point F. On the other hand, the results of the observation point B show non-physical high frequent oscillation in the total component and the far-field component. The isochrones formula Eq. (11) shows that the isochrones band is dominant for ground motion estimation. Especially the width of the isochrones band is proportional to  $|\nabla\theta(\varphi^t(\lambda'))|^{-1}$ . Fig 4 shows that the isochrones band width of the backward directivity is less than that of the forward directivity because the norm of  $\nabla\theta$  of the backward directivity is greater than that of the forward directivity. From these results we found that numerical instabilities are caused when the mesh size is larger than the isochrones band width. Actually we can avoid the numerical instabilities from the backward directivity case by using the fine mesh which is smaller than one third of the isochrones band width.

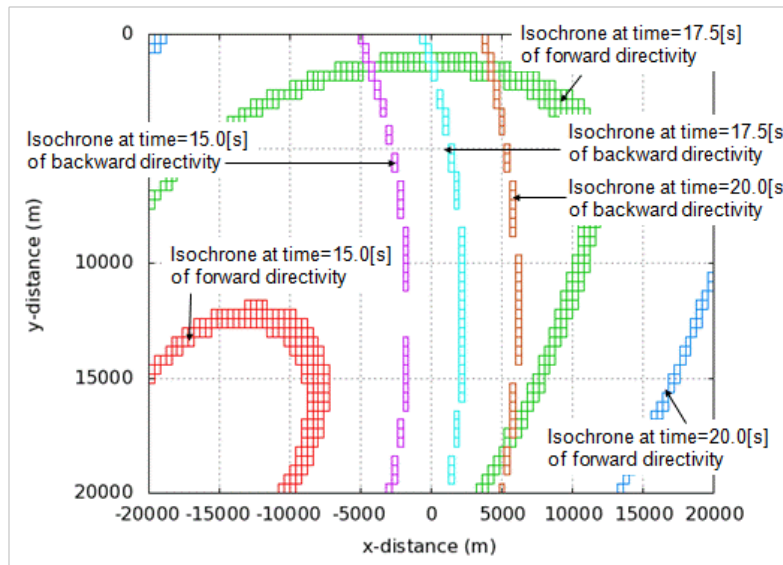


Fig 4. Shapes of the isochrones band

Red : isochrones band of the forward directivity at 15.0[s]  
 Green : isochrones band of the forward directivity at 17.5[s]  
 Blue : isochrones band of the forward directivity at 20.0[s]  
 Pink : isochrones band of the backward directivity at 15.0[s]  
 Cyan : isochrones band of the backward directivity at 17.5[s]  
 Brown: isochrones band of the backward directivity at 20.0[s]

### 3.2 Ground motion simulations with non-uniform rupture velocity

Next we show some parametric studies of the ground motion simulation with non-uniform rupture velocity. We consider the M7 class earthquake to set some fault parameters by following the recipe [10]. The fault width and length are 20km and 20km respectively. The asperity region is a square with length of 8km. We let the rupture velocity of the asperity region and the background region to be  $0.72\beta$  and that of the margin region to be  $0.30\beta$ . ( $\beta$  is the secondary wave velocity) Then our eikonal solver gives rupture delay times for the fault model.

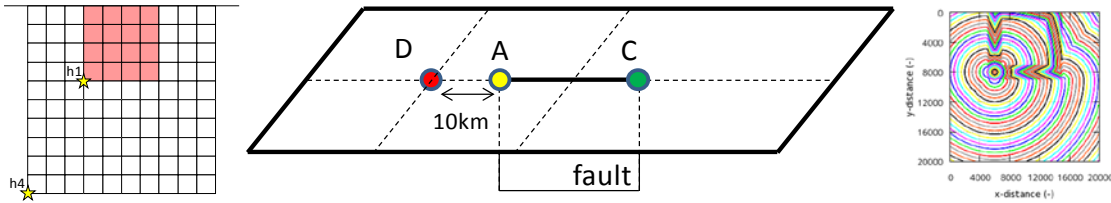


Fig 5. Asperity and hypocenter in a fault model (left and center) and rupture delay time (right)

An asperity region is marked by pink color and a background region is marked by white color. Star symbol stands for positions of hypocenter. Three observation points are located on the plane which includes the upper edge of the fault and is perpendicular to it.

In what follows, some results of the point A are given. The point A means a typical position of the backward directivity. First we investigate time histories of ground velocity of the backward directivity point. Compared with cases of the uniform rupture velocity and the non-uniform rupture velocity, it turns out that more pulse-like disturbance of velocity waveform of ground motion appears in the case of the non-uniform rupture velocity. In order to discuss some relations between the pulse-like disturbance of ground motion and isochrones band, we investigate time histories of the rate of change of isochrones band area. Fig 7 shows that the rate of change of the isochrones band area in the case of non-uniform rupture velocity has more pulse-like disturbance. Fig 8 shows that the isochrones band is deformed when it crosses the boundary on which the rupture velocity varies. We will discuss these pulse-like disturbance in the section 4.

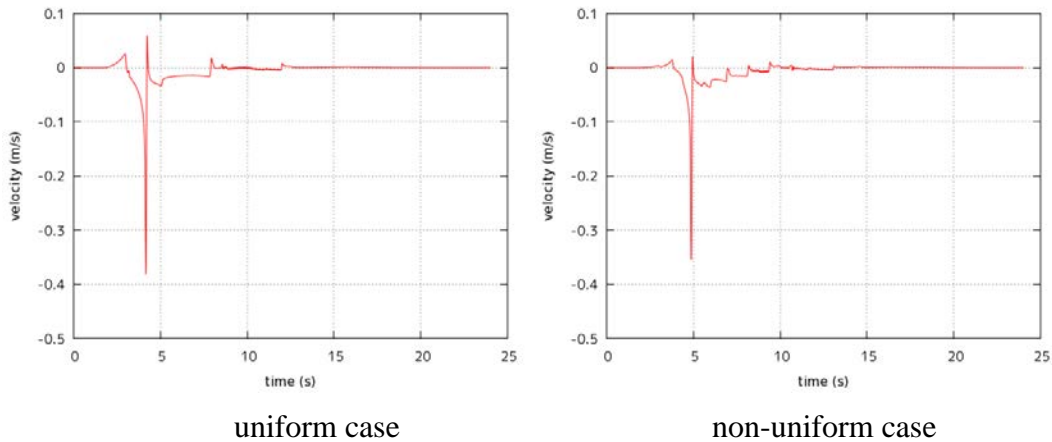


Fig 6. Time histories of ground motion velocity at the backward directivity point

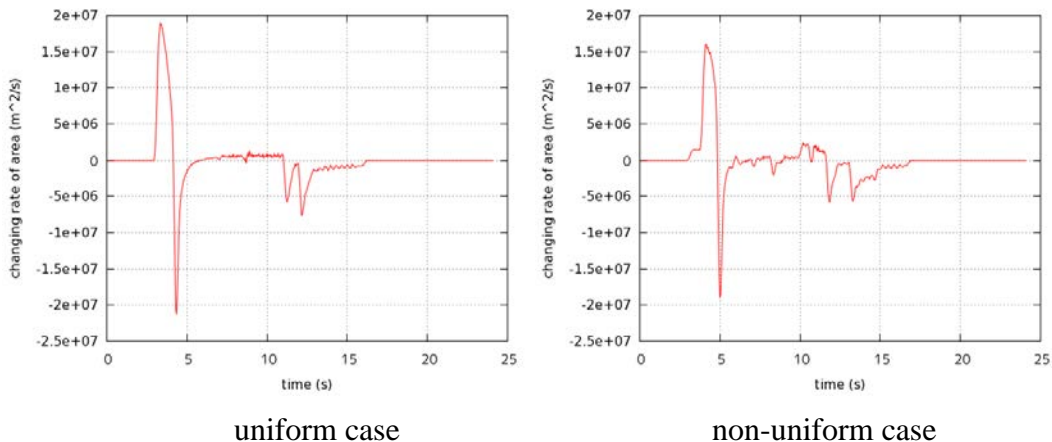


Fig 7. Time histories of rate of change of isochrones band area at the backward directivity

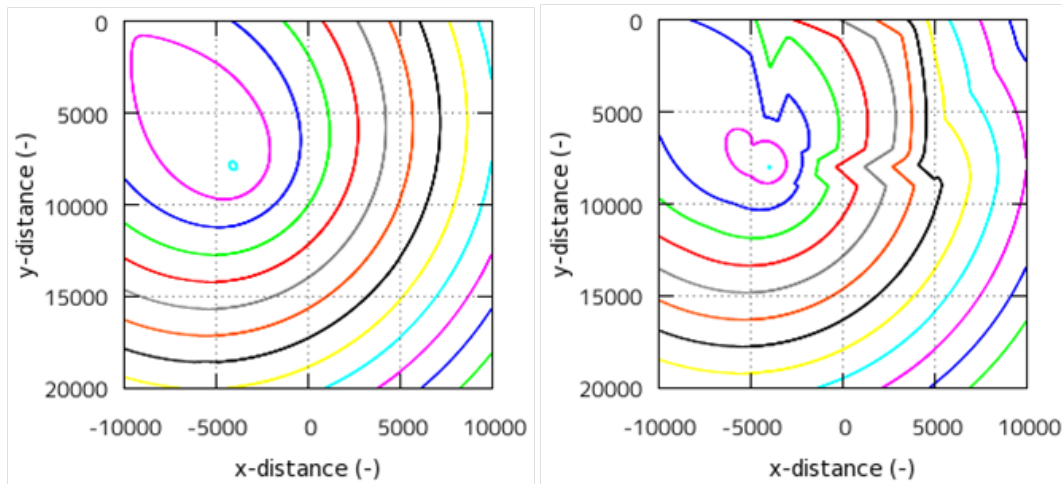
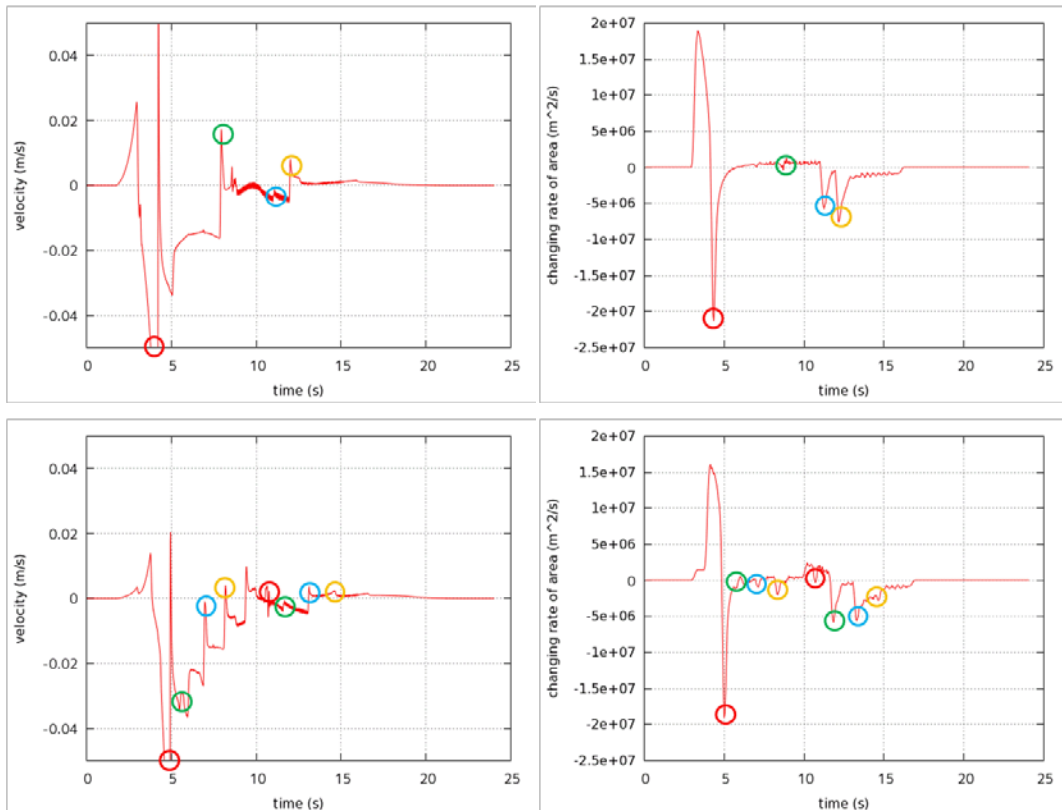


Fig 8. Isochrones bands every one second w.r.t. the backward directivity point

#### 4. Discussions

As shown in the section 3.2, the pulse-like disturbance of ground motion velocity corresponds to that of rate of change of isochrones band area. Especially the timing of disturbance of ground motion velocity coincides with that of rate of change of isochrones band area. In the figure below we marked up the timing of disturbance of the graphs in Fig 6 and Fig 7 to compare with each others.



ground velocity

rate of change of isochrones band area

Fig 9. Zoom up of Fig 6 and Fig 7 : Comparison of ground velocity and rate of change of isochrones band area

$$\left[ \begin{array}{l} \text{Upper: the case of uniform rupture velocity} \\ \text{Lower : the case of non-uniform rupture velocity} \end{array} \right]$$

Now we explain this coincidence of the timing for disturbances of velocity waveform of ground motion and rate of change of isochrones band area. Using the isochrones jumping intensity and the decomposed isochrones formula Eq. (15), we can distinguish the disturbance component  $V_{dis}$  of velocity waveform of ground motion.

$$V_{dis}(t) = \int_0^1 j_h(\lambda') f(t - \tau(\lambda')) d\lambda', \quad (16)$$

$$h_{\lambda'}(t) = g(\varphi^t(\lambda')) |\nabla\theta(\varphi^t(\lambda'))|^{-1} \left| \frac{d\varphi^t}{d\lambda'} \right|,$$

where the integrand  $j_h(\lambda') = h_{\lambda'}(\tau + 0) - h_{\lambda'}(\tau - 0)$  is the isochrones jumping intensity and  $f(t)$  is a slip velocity function  $\dot{F}(t)$ . The same argument derives the disturbance component  $A_{dis}$  of rate of change of isochrones band area.

$$A_{dis}(t) = \int_0^1 j_H(\lambda') f(t - \tau(\lambda')) d\lambda', \quad (17)$$

$$H_{\lambda'}(t) = |\nabla\theta(\varphi^t(\lambda'))|^{-1} \left| \frac{d\varphi^t}{d\lambda'} \right|,$$

where the integrand  $j_H(\lambda') = H_{\lambda'}(\tau + 0) - H_{\lambda'}(\tau - 0)$  is a modified isochrones jumping intensity with  $g(\xi) \equiv 1$ . These expressions of  $V_{dis}$  and  $A_{dis}$  means that the disturbance of them occurs at the same timing  $t = \tau(\lambda')$ . That is to say, it occurs when the isochrones jumping intensity has nonzero value.

## 5. Conclusion

For the purpose of evaluating variability of ground motion prediction, we had three achievements for a ground motion simulation. First, in order to deal with a curved surface fault with spatially discontinuous non-uniform rupture propagation velocity, we proposed a kinematic modelling in which the rupture delay time is governed by the eikonal equation on Riemannian manifold and developed a coupling method between the eikonal solver on Riemannian manifold and a ground motion simulation. Next, in order to explain the effect of spatially discontinuous non-uniformity of rupture velocity, we introduced an isochrones jumping intensity and obtained a new decomposed isochrones formula for ground velocity. Finally, by applying our coupling method and decomposed isochrones formula we explained that the pulse-like disturbance of the ground velocity occurs when the isochrones jumping intensity has nonzero value. Moreover we showed a characteristic dependency of peak ground velocity upon parameters such as rupture velocity and distance between the fault and observer.

We, however, think that further discussion with respect to the decision of rupture velocity is required. So we would like to study the dynamic rupture model in order to understand how to give the spatial distribution of rupture velocity in future works.

## 5. References

- [1] Bizzarri, A., Analytical representation of the fault slip velocity from spontaneous dynamic earthquake models, *J. Geophys. Res.*, Vol.117, 2012
- [2] H. Nakamura and T. Miyatake, An approximate expression of slip velocity functions for simulation of near-field strong ground motion, *Zisin (J Seism Soc Japan)* 53, pp.1-9 (in Japanese), 2000
- [3] Benard, P. and R. Madariaga, A new Asymptotic Method for the Modeling of Near-Field Accelerograms, *Bull. Seismol. Soc. Am.*, Vol.74, No.2, pp.539-557, April 1984

- [4] Spudich, P. and Frazer L. N., Use of ray theory to calculate highfrequency radiation from earthquake sources having spatially variable rupture velocity and stress drop, *Bull. Seismol. Soc. Am.*, 74, 2061-2082, 1984
- [5] Bizzarri, A. and Spudich, P., Effects of supershear rupture speed on the high-frequency content of S waves investigated using spontaneous dynamic rupture models and isochrones theory, *J. Geophys. Res.*, 113, 2008
- [6] J. A. Sethian, *Level Set Methods and Fast Marching Methods: Evolving Interfaces in Computational Geometry, Fluid Mechanics, Computer Vision, and Materials Science*, Cambridge University Press, 1999
- [7] J. A. Sethian and A. Mihari Popovici, 3-d travelttime computation using the fast marching method, *Geophysics*, 64 (2), 516-523, 1999
- [8] Spirall, A. and Kimmel, R., An efficient solution to the eikonal equation on parametric manifolds, *Interfaces and Free Boundaries*, 6 (2004), 315-327
- [9] Aki, K. and P. G. Richard, *Quantitative seismology*, Theory and Methods, W. H. Freeman and company, San Francisco, 1980
- [10] Irikura, K. and H. Miyake, Source Modeling for Ground Motion Prediction, *Chikyu Monthly*, Extra No.37, pp.62-77, 2002